ECOLE DES MINES DE NANTES

SUBATECH

UMR Université, Ecole des Mines, IN2P3/CNRS

LABORATOIRE DE PHYSIQUE SUBATOMIQUE
ET DES TECHNOLOGIES ASSOCIEES

ROTATING BUBBLE AND TOROIDAL NUCLEI AND FRAGMENTATION

G. Royer, F Haddad and B. Jouault

Rapport Interne SUBATECH -95-17

4, RUE ALFRED KASTLER. LA CHANTRERIE. 44070 NANTES CEDEX 03. TELEPHONE 51 85 81 00. TELECOPIE 51 85 84 79. E-mail : @ FRCPN11.IN2P3.FR

ROTATING BUBBLE AND TOROIDAL NUCLEI AND FRAGMENTATION

G. Royer, F. Haddad and B. Jouault

Laboratoire de physique subatomique et des technologies associées
UMR : IN2P3/CNRS, Université et Ecole des Mines de Nantes
4 rue A.Kastler, La Chantrerie - 44070 - Nantes-Cedex 03 - France

Abstract : The energy of rotating bubble and toroidal nuclei predicted to be formed in central heavy-ion collisions at intermediate energies is calculated within the generalized rotating liquid drop model. The potential barriers standing in these exotic deformation paths are compared with the three dimensional and plane fragmentation barriers. Metastable bubble-like minima only appear at very high angular momentum and above the three dimensional fragmentation barriers. In the toroidal deformation path of the heaviest systems exists a large potential pocket localised below the plane fragmentation barriers. This might allow the temporary survival of heavy nuclear toroids before the final clusterisation induced by the surface and proximity tension.

1.Introduction

Heavy-ion central collisions above a few tens of MeV per nucleon allow to produce hot and compressed nuclear matter. The breakup of the system into several intermediate mass fragments (IMF) is an important part of the reaction cross section. A large number of experimental [1-6] and theoretical [7-12] works have been performed to unravel the underlying physics responsible for this fragmentation in central reactions. In peripheral collisions, multiple neck rupture is also an efficient IMF production mechanism [13].

The predicted number of intermediate mass fragments produced assuming homogeneously filled spherical source is lower than the experimentally observed one. Moreover, simulations based on microscopic semi-classical models [14-18], temperature time dependent Hartree-Fock approach [19] and hydrodynamical calculations [20] predict the formation of exotic nuclear shapes like disks, toroids and bubbles just after the most violent phase of central heavy-ion collisions and prior to fragmentation. The energy threshold for this type of fragmentation from unstable hollow configurations seems to be around 50 MeV/u for medium systems [14] and only 30 MeV/u for the heaviest systems [5,17,21] due to their fundamental instability. Then the observed enhanced production of IMF might be explained by the Coulomb and isospin effects [12,17] which drive the decay path toward exotic shapes where the interfragment Coulomb interaction energy is smaller increasing the likelyhood of a multifragment disintegration. This effect increases with the symmetry of the reaction since it optimizes the compression and Coulomb effects. Experimentally, remarkably flatness of the charge distribution [21] and observation of IMF emitted almost in the same plane [22] are the first preliminary indications of the existence of such evanescent exotic configurations. To delineate the different fragmenting configurations it has been suggested to exploit the differences in the inclusive charge distributions via the IMF-IMF correlation functions [23] but it is possible that collective rotation dictates the focusing of decay patterns into the plane perpendicular to the total angular momentum.

The purpose of the present work is to compare the macroscopic deformation energy of the bubble and toroidal nuclei to the potential barriers of fragmentation into several spherical nuclei emitted in a volume-like manner and in a ring-like manner. The purpose is to know to what extent bubble-like and toroidal nuclear systems might temporary exist before fragmenting due to the influence of the surface tension and proximity forces. At first, in sect.2, are displayed the results of a simulation within the microscopic dynamic landau-Vlasov model indicating the fragment formation in the thick skin of an expanded nuclear system with a central matter depression. The geometric characteristics of bubbles, toroids and different fragmentation configurations are given in sect.3. In sect.4, the dependence of the bubble-like and toroidal deformation barriers on the rotation, temperature and mass are determined. Finally, the potential energies in these different exotic exit channels are compared in sect.5.

2. IMF emission in the ^{208}Pb(29 MeV/u) + ^{197}Au reaction at b = 2 fm

The Pb(29 MeV/u) + Au and Au(35 MeV/u) + Au reactions have been recently studied [5,21,24] and the emission of several IMF has been observed in central collisions. Landau-Vlasov simulations [17] predict the existence of four phases in the central reactions. In a first phase, the overlap region is strongly compressed and, later on, the whole system is very compact. Secondly, due to the Coulomb repulsion and saturation of the nuclear forces, the system expands rapidly. In a third phase the nuclear matter contracts at the vicinity of the

external surface and a depletion grows in the centre of the system while the external expansion slowly continues. This central depression appears in all planes containing the centre of mass. The repartition of the surrounding nucleons is very inhomogeneous but nevertheless rather of volume-like type both for soft and stiff equations of state. Finally instabilities due to the surface and proximity forces develop clusterizing the thick skin of the hollow system into several massive fragments (see figure 1). This clusterization clearly occurs at around 150-250 fm/c as seen in figure 2 where each column gives the repartition of the matter which finally will constitute one of the fragments (a time reversal procedure has been used).

In such a picture, the fragmentation is neither uniquely sequential nor simultaneous from a compact filled spherical source. It is rather simultaneous from an expanded and hollow source without excluding some sequentiality since some hot distorted heavy fragments undergo binary and ternary fission later on.

3.Geometric characteristics of bubbles, toroids and different fragmentation configurations

Macroscopic approaches complete the microscopic semi-classical models in providing rapidly estimates of the main observables as potential energy, angular momentum, kinetic energy, temperature, mass and asymmetry dependence, ...Then, the nuclei are considered as classical systems endowed with uniform charge and mass densities and a surface tension. The compression, the inhomogeneities and the out of equilibrium effects introduced by the dynamics in the violent heavy-ion collisions are naturally not taken into account and such calculations give only preliminary quantitative informations. Nevertheless, they are railings for further investigations.

The exotic exit channels corresponding to bubble and toroidal shapes and plane and three dimensional emission of several fragments have been studied within the macroscopic rotating liquid-drop model including the nuclear proximity energy and the temperature. Assuming volume conservation, the bubble characteristics can be expressed in terms of a single variable, the ratio $p = r_1/r_2$ of the inner radius r_1 and the outer radius r_2.

$$V = \frac{4}{3}\pi R_0^3 = \frac{4}{3}\pi(r_2^3 - r_1^3), \tag{3.1}$$

$$r_2 = R_0(1-p^3)^{-1/3}, \tag{3.2}$$

$$r_1 = R_0 p(1-p^3)^{-1/3}. \tag{3.3}$$

The relative (to the sphere) root mean square radius is given by :

$$< r^2 >_{rel}^{1/2} = \frac{< r^2 >^{1/2}}{\sqrt{\frac{3}{5}}R_0} = (1-p^5)^{1/2}(1-p^3)^{-5/6}. \tag{3.4}$$

The dependence of the r.m.s radius on the ratio r_1/r_2 is displayed in figure 3. The r.m.s radius increases slowly with the deformation because of the isotropic expansion in the whole three dimensional space.

The relative moment of inertia and surface and Coulomb energies read [25] :

$$I_{\perp rel} = \frac{I_\perp}{\frac{2}{5}mR_0^2} = (1-p^5)(1-p^3)^{-5/3}, \tag{3.5}$$

$$B_s = \frac{1+p^2}{(1-p^3)^{2/3}}, \tag{3.6}$$

$$B_c = \frac{1-2.5p^3+1.5p^5}{(1-p^3)^{5/3}}. \tag{3.7}$$

The toroidal deformation path has been studied using the one parameter shape sequence recently defined [26]. It leads continuously from a sphere towards a pumpkin-like configuration (oblate elliptic lemniscatoids) and, later on, to an holed torus. Analytical expressions are available for the shape dependent functions except for the Coulomb function calculated within the Wong's formula [27].

The emission of 2, 3, 4, 6 and 8 equal spherical fragments in a volume and ring-like manner has been described in putting the mass centres on the tops of symmetric configurations : equilateral triangle, tetrahedron, octahedron and cube in the first case and square, hexagon and octogon for the plane fragmentation [28-29]. The two fragment emission has been studied from the initial sphere within a compact and creviced shape sequence (prolate elliptic lemniscatoids) leading rapidly to two tangent spherical nuclei and already used to investigate the binary fission [30]. The mean square radius of these distributions is related to the distance l from the centre of each fragment to the mass centre of the total system by

$$< r^2 >= \frac{3}{5} R_0^2 n^{-2/3} + l^2. \tag{3.8}$$

The relative moment of inertia in the different exit channels are compared in figure 4. For a given r.m.s radius, the moment of inertia of a bubble is smaller than the one of a compact and creviced shape since much more matter remains close to the rotation axis. The toroidal shape is the most efficient to keep away the nucleon distribution from the perpendicular symmetry axis and, then, to maximize the moment of inertia. On the other hand, the total (inner and outer) surface of a bubble increases more rapidly than the surface of a torus (see figure 5) and the surface of binary elongated shape since the deformations occur respectively in the three dimensional space, in a plane and on an axis. For n equal separated spherical fragments the surface naturally is constant and proportional to $n^{1/3}$ assuming volume conservation. The three dimensional fragmentation corresponds to more compact configurations and, then, to lower values of the r.m.s radius. For 4, 6 and 8 fragments close to the contact point the surface energy is close to the bubble one. The figure 6 indicates that the bubble shape is the most efficient to minimize the Coulomb repulsion, comes after the toroid and finally the binary decay channel. The reason lies also in the respective three, two and one spatial deformation degrees of freedom. The Coulomb functions of the plane and three dimensional fragment emission approach to the ones of the toroid and the bubble with increasing number of fragments.

4.Energy of rotating hot bubble and toroidal nuclei

Assuming constant density, the macroscopic deformation energy of a hot nuclear system with gaps and crevices is the difference between the Coulomb, surface and proximity energies of the deformed system and the ones of the initial spherical nucleus :

$$E_{def} = \frac{3e^2Z^2}{5R_0}(B_c - 1) + a_s(1-2.6I^2)A^{2/3}(B_s - 1) + E_{prox}, \tag{4.1}$$

where A, Z and I are the mass, charge and relative neutron excess. The proximity energy takes into account the nuclear attraction between surfaces in regard of distorted shapes and

supplements the surface energy which derives from the integration of the superficial tension forces in an half-space.

The temperature dependent effective sharp radius R_0 and surface coefficient a_s have been choosen as

$$R_0=(1.28A^{1/3}-0.76+0.8A^{-1/3})(1+0.0007T^2)\ \text{fm}, \quad (4.2)$$

$$a_S=17.9439(1+1.5T/17)(1-T/17)^{3/2}\ \text{MeV}. \quad (4.3)$$

For a given angular momentum, the rotational energy is given by :

$$E_{rot}=\frac{\hbar^2 l(l+1)}{2I_\perp} \quad (4.4)$$

where $I_\perp$ is the rigid perpendicular moment of inertia.

The bubble-like and toroidal deformation barriers for the rotating ^{96}Mo, ^{208}Pb nuclei and ^{400}147 nuclear system are displayed in figures 7, 8 and 9. In the whole mass range, a very high potential barrier stands in the bubble-like deformation path. This is mainly due to the rapid increase of the surface. The introduction of a rotational energy does not allow to lower rapidly the barrier since the moment of inertia increases slowly with the deformation. Therefore, a potential pocket appears only at very large angular momenta. The temperature slightly reduces the potential energy and deformed minima appear at lower angular momenta. As an example, at T = 7 MeV and for the heaviest system, metastable minima corresponding roughly to $<r^2>_{rel}^{1/2}\approx 1.15$ and $r_i\approx 5$ fm exist for l > 250-300 $\hbar$. The r_i value is approximately comparable with the hole radius of the very inhomogeneous bubble formed in the Pb (29 MeV/u) + Au reaction at b = 2 fm which leads to an angular momentum of around 230 $\hbar$.

The toroidal deformation barriers are always lower than the bubble ones but, nevertheless, they are also very high in the whole periodic table since the torus surface augments infinitely with its radius. With increasing mass and/or angular momenta the potential barriers present two wells. The first one roughly correponds to a torus the radius of which is equal to the sausage radius. The second one is very large. The inner minima disappears at the highest angular momenta while the outer one is pushed to larger deformations. At T = 6-7 MeV and for A > 220 (see also [26]) the outer potential pocket already appears at l = 0.

Such a rough macroscopic approach seems to indicate that the very inhomogeneous "bubble of nuclear magma" formed in very massive heavy-ion collisions at intermediate energies should rapidly evolve into rather plane toroidal configurations.

5.Bubble and toroidal deformation paths and three dimensional and plane fragmentation

The deformation energy in the bubble and toroidal shape paths are compared in figures 10, 11 and 12 with the three dimensional and plane fragmentation barriers encountered by n equal fragments symmetrically arranged on regular polyhedral and polygonal configurations. In the one-body exit channels the barrier standing against deformations rises infinitely. This is the main reason of the extreme instability of these exotic shapes and this definitively forbids the evolution of the system towards very large bubbles or torii. In contrast, in the multi-fragmentation channels, smoothly appears a saddle-point and, later on, a steep slope of the potential energy. The saddle-point corresponds to n separated fragments held together by the balance between the repulsive Coulomb forces and the attractive nuclear ones. As a quantitative illustration, the proximity energy respectively reaches -292 and - 202 MeV at the contact point and - 30 and - 25 MeV at the saddle-point

for cubic and octogonal configurations for the ^{208}Pb nucleus at T = 0. This clearly points out the extreme importance of this contribution to the total energy when the nuclear systems are strongly distorted.

The plane fragmentation barriers are always lower than the three dimensional ones. The barrier heights increase with the fragment number except for the case of the plane emission from the heaviest systems. The three dimensional fragmentation barriers are well below the bubble-like deformation barriers whatever is the mass and the temperature of the system. So, it seems that metastable rotating bubble-like states are very evanescent configurations. On the contrary, the deep and wide potential pocket which progressively appears with increasing mass in the toroidal shape exit channel is located below the potential barriers of the multi-fragment plane emission at least in some deformation range. This might justify the temporary survival of a metastable toroidal state before its decay in the multifragment exit channels due to the action of the surface tension and proximity forces which tend to minimize the potential energy in clusterizing the matter distribution.

6.Conclusion

The bubble and toroidal nuclei predicted to be formed in heavy-ion central collisions at intermediate energies are investigated within the generalized rotating liquid drop model taking into account both the temperature and the nuclear proximity energy. The surface increases quickly and indefinitely with the deformation for the two configurations but much more rapidly for the bubble nuclei. In contrast, the moment of inertia increases more slowly for the bubbles than for the torii. Consequently, high and steep potential barriers stand in the two paths but toroidal shapes are more favoured and, furthermore, the introduction of the rotational energy is more effective to lower the toroidal deformation barriers than the bubble ones.

Metastable bubble-like minima only appear at very high angular momenta and above the barriers of three dimensional multifragmentation. In the toroidal deformation path of very heavy systems accessible as residues in heavy-ion reactions exists a large potential pocket localised below the plane fragmentation barriers for some deformation range. If the dynamics in the most massive central heavy-ion collisions leads the nuclear system to very distorted rotating hollow bubble configurations after the compression phase the system will afterwards evolve rather to evanescent toroidal matter distributions while clusterising under the action of the surface tension and proximity forces.

Acknowledgments :
We take pleasure in thanking F. Sebille for fruitful discussions, C. Fauchard for wide use of his program and V. Moreau and M. Rio for performing the figures.

REFERENCES

[1] Y.D. Kim et al, Phys. Rev. Lett. 63 (1989) 494
[2] D.Cebra et al, Phys. Rev. Lett. 64 (1990) 2246
[3] Y.Blumenfeld et al, Phys. Rev. Lett. 66 (1991) 576
[4] D.R. Bowman et al, Phys. Rev. C 46 (1992) 1834
[5] J.F. Lecolley et al, Phys. Lett. B 325 (1994) 317
[6] W.G. Lynch, Nucl. Phys. A 583 (1995) 471c
[7] G.F. Bertsch, H. Kruse and S. Das Gupta, Phys. Rev. C 29 (1984) 673
[8] J.P. Bondorf, R. Donangelo, I.N. Mishustin and H. Schultz, Nucl. Phys. A 444 (1985) 460
[9] L. Vinet, C.Gregoire, P. Schuck, B. Remaud and F. Sebille, Nucl. Phys. A 468 (1987) 321
[10] G.Peilert, H. Stöcker, W. Greiner, A. Rosenhauer, A. Bohnet and J. Aichelin, Phys. Rev. C39 (1989) 1402
[11] J. Richert and P. Wagner, Nucl. Phys. A 517 (1990) 399
[12] D. H. E. Gross, Rep. Prog. Phys. 53 (1990) 605
[13] J. Toke et al, Phys. Rev. Lett. 75 (1995) 2920
[14] W. Bauer, G. F. Bertsch and H.Schulz, Phys. Rev. Lett. 69 (1992) 1888
[15] L.G. Moretto, Kin Tso, N. Colonna and G.J. Wozniak, Phys. Rev. Lett. 69 (1992) 1884
[16] S.R. Souza and C. Ngô, Phys. Rev. C 48 (1993) R2555
[17] B. Jouault, F. Sebille, G. Royer and V. de la Mota, Nucl. Phys. A 591 (1995) 497
[18] H.M. Xu, C.A. Gagliardi, R.E. Tribble and C.Y. Wong, Nucl. Phys. A 569 (1994) 575
[19] H. Ngô, F.Z. Ighezou, C. Ngô, J. Nemeth and L. Depaola, XXI Workshop on gross properties of nuclei and nuclear excitations, Hirschegg, Austria 1993 (GSI, Darmstadt, 1993) 302
[20] C.E. Aguiar, R. Donangelo, C.O. Dorso, R.S. Gomes and N. Gonçalves, Phys. Rev. C 46 (1992) 1069
[21] M. D'Agostino et al, preprint MSUCL 975 (1995)
[22] D. Durand, Ganil symposium " Advances in nuclear physics", Le Pradet, France, (1995)
[23] S. Pal, S.K. Samaddar and J.N. De, Nucl. Phys. A 589 (1995) 489
[24] R. Bougault et al, Nucl. Phys. A 587 (1995) 499
[25] C.Y. Wong, Ann. of Phys. 77 (1973) 279
[26] C.Fauchard and G.Royer, Nucl. Phys. A (1995) in print
[27] C.Y. Wong, Phys. Rev. C 17 (1978) 331
[28] F. Haddad and G. Royer, J. of Phys. G18 (1992) L153
[29] G. Royer and F. Haddad, J. of Phys. G20 (1994) L131
[30] G. Royer and B. Remaud, J. of Phys. G10 (1984) 1057

FIGURE CAPTIONS

Figure 1 : Time evolution of the nuclear densities in the reaction plane in the ^{208}Pb(29 MeV/u) + ^{197}Au reaction at b = 2 fm. The time (fm/c unit) is given in the right upper corner of each panel. The horizontal and vertical coordinates are in fm. The two last rows show the projected densities in the reaction plane.

Figure 2 : Time evolution of the projected nuclear densities of each future fragment emitted in the ^{208}Pb(29 MeV/u) + ^{197}Au reaction at b = 2 fm.

Figure 3 : Relation between the relative root mean square radius of the matter distribution and the ratio r_1/r_2 of the bubble radii.

Figure 4 : Relative moment of inertia of a bubble and a toroid (full lines) and of compact binary fission shape (dashed line) as a function of the relative root mean square radius.

Figure 5 : Relative surface energy of a bubble and a toroid (full lines) and of plane (dashed lines) and three dimensional (dashed and dotted) configurations leading to 2,3, 4, 6 and 8 equal spherical fragments.

Figure 6 : Relative Coulomb energy of a bubble and a toroid (full lines) and of plane (dashed lines) and three dimensional (dashed and dotted) configurations leading to 2,3, 4 and 6 equal spherical fragments.

Figure 7 : Sum of the deformation and rotational energies at T = 0 and 7 MeV as functions of the r.m.s radius and angular momentum ($\hbar$ unit) for ^{96}Mo for the bubble and toroidal nuclear configurations.

Figure 8 : Same as figure 7 but for ^{208}Pb.

Figure 9 : Same as figure 7 but for ^{400}147.

Figure 10 : Comparison at T = 0 and T = 7 MeV between the bubble deformation barrier (full curve) and barriers of three dimensional emission (dashed curves) and between the toroidal deformation barrier (full curve) and barriers of plane fragmentation (dashed curves) for ^{96}Mo.

Figure 11 : Same as figure 10 but for ^{208}Pb.

Figure 12 : Same as figure 10 but for ^{400}147.

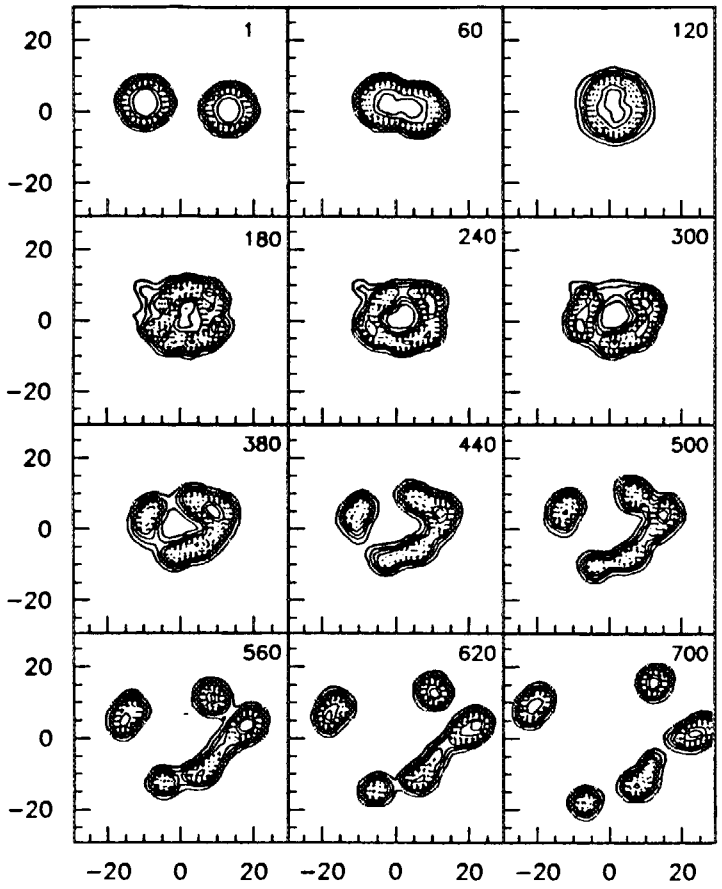

Figure 1

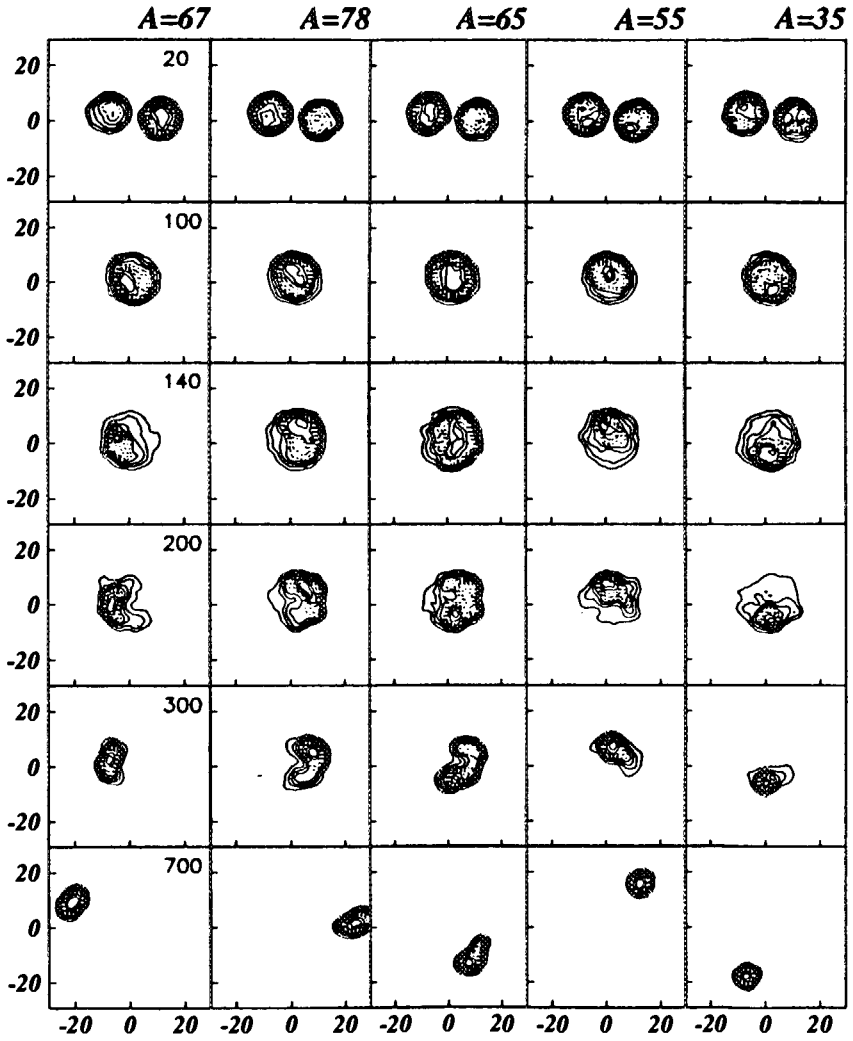

Figure 2

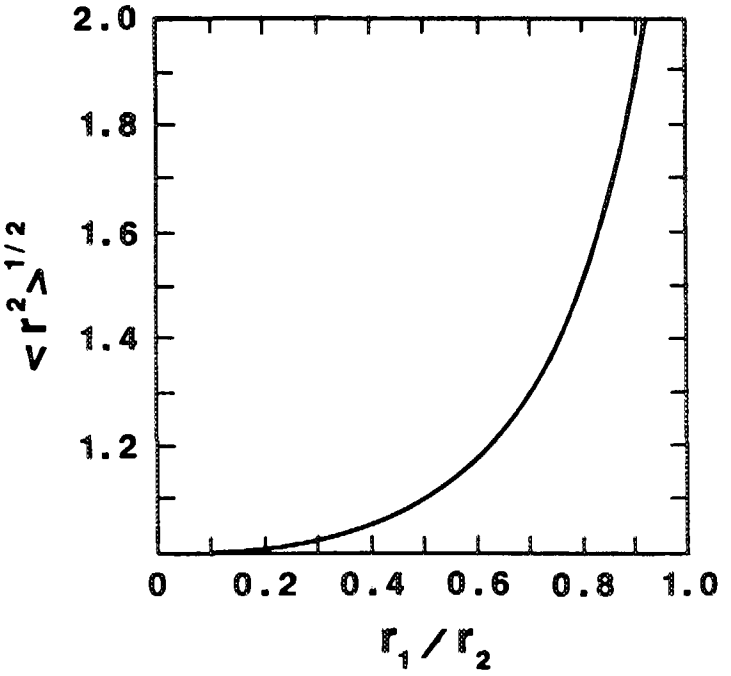

Figure 3

Figure 4

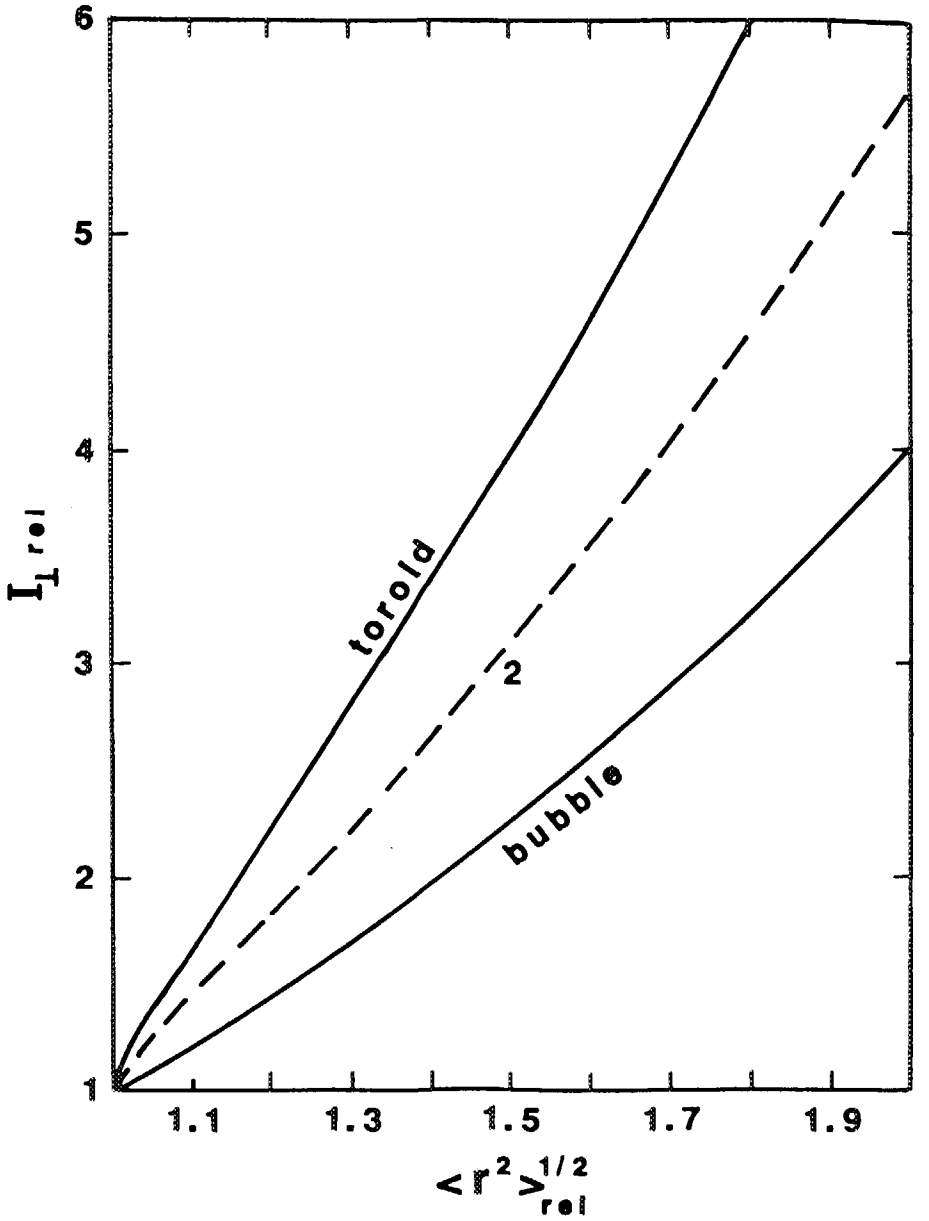

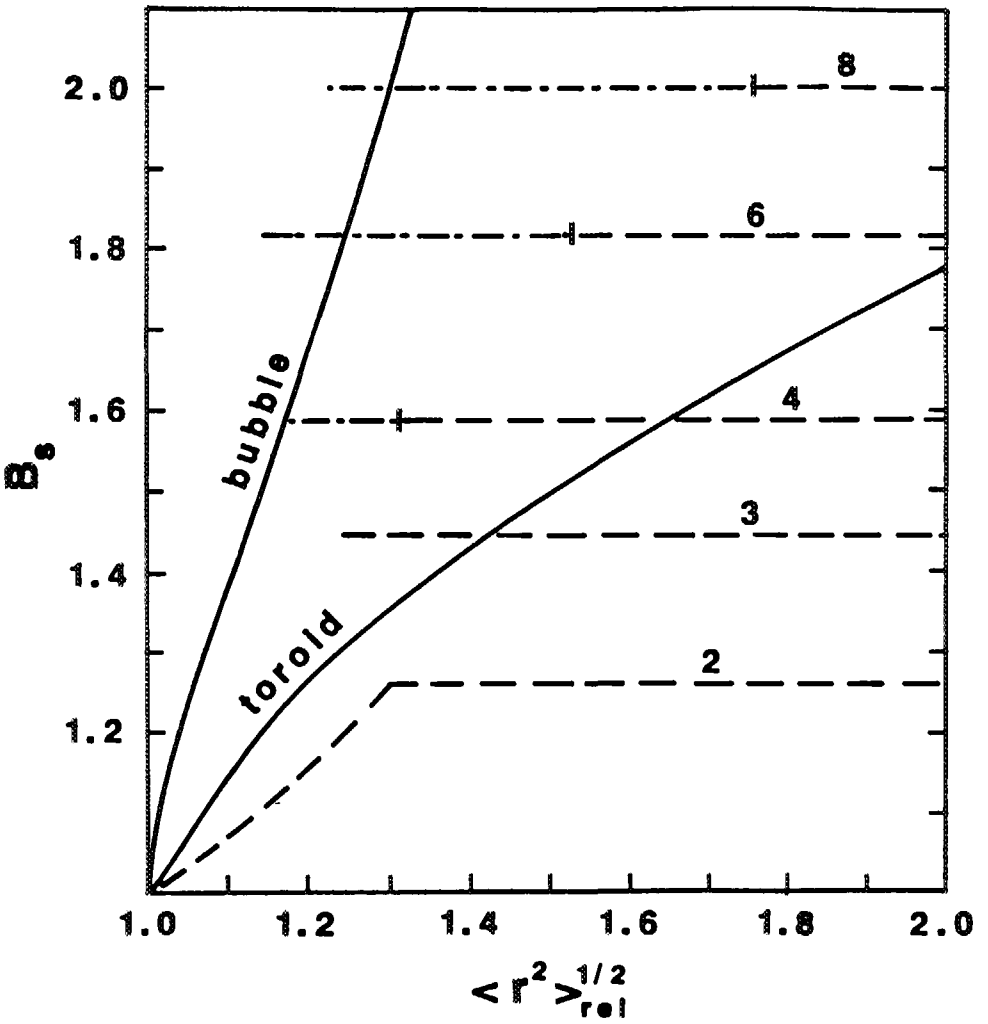

Figure 5

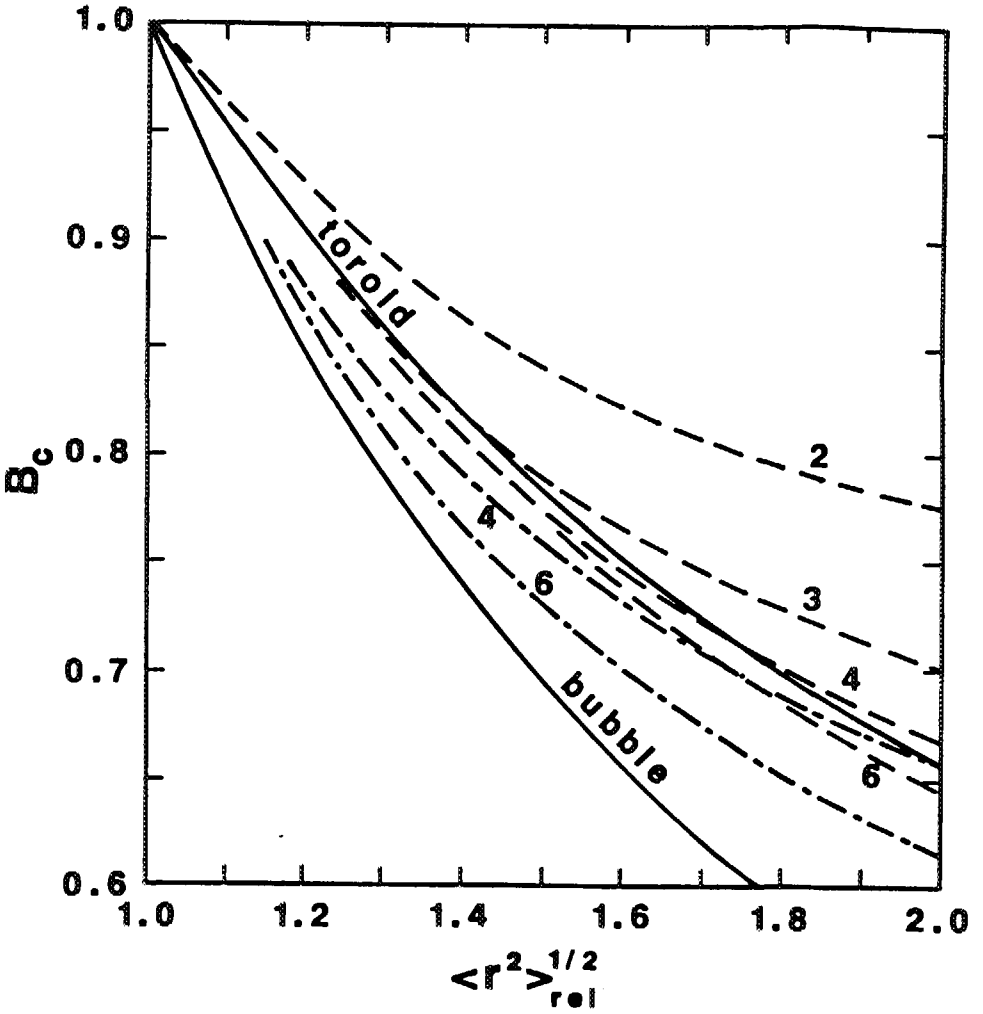

Figure 6

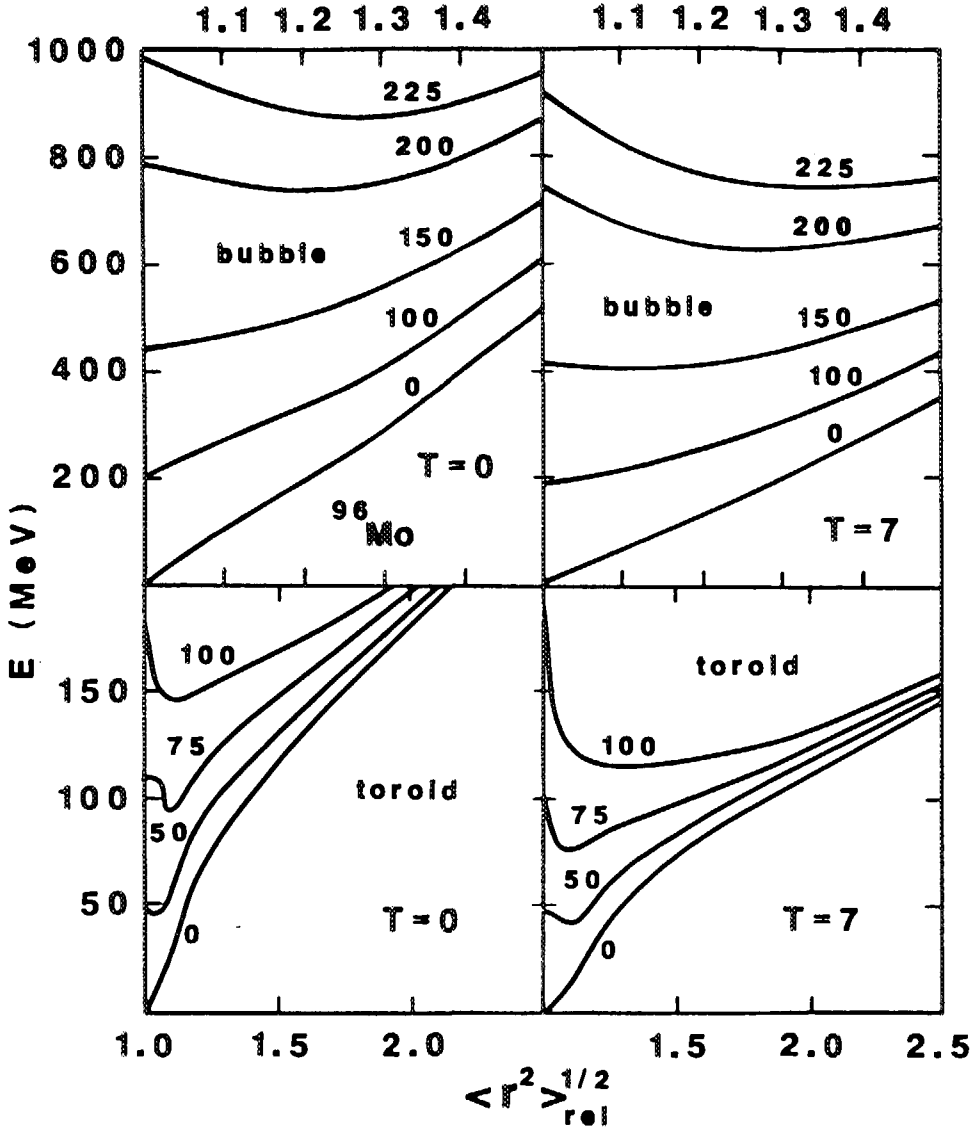

Figure 7

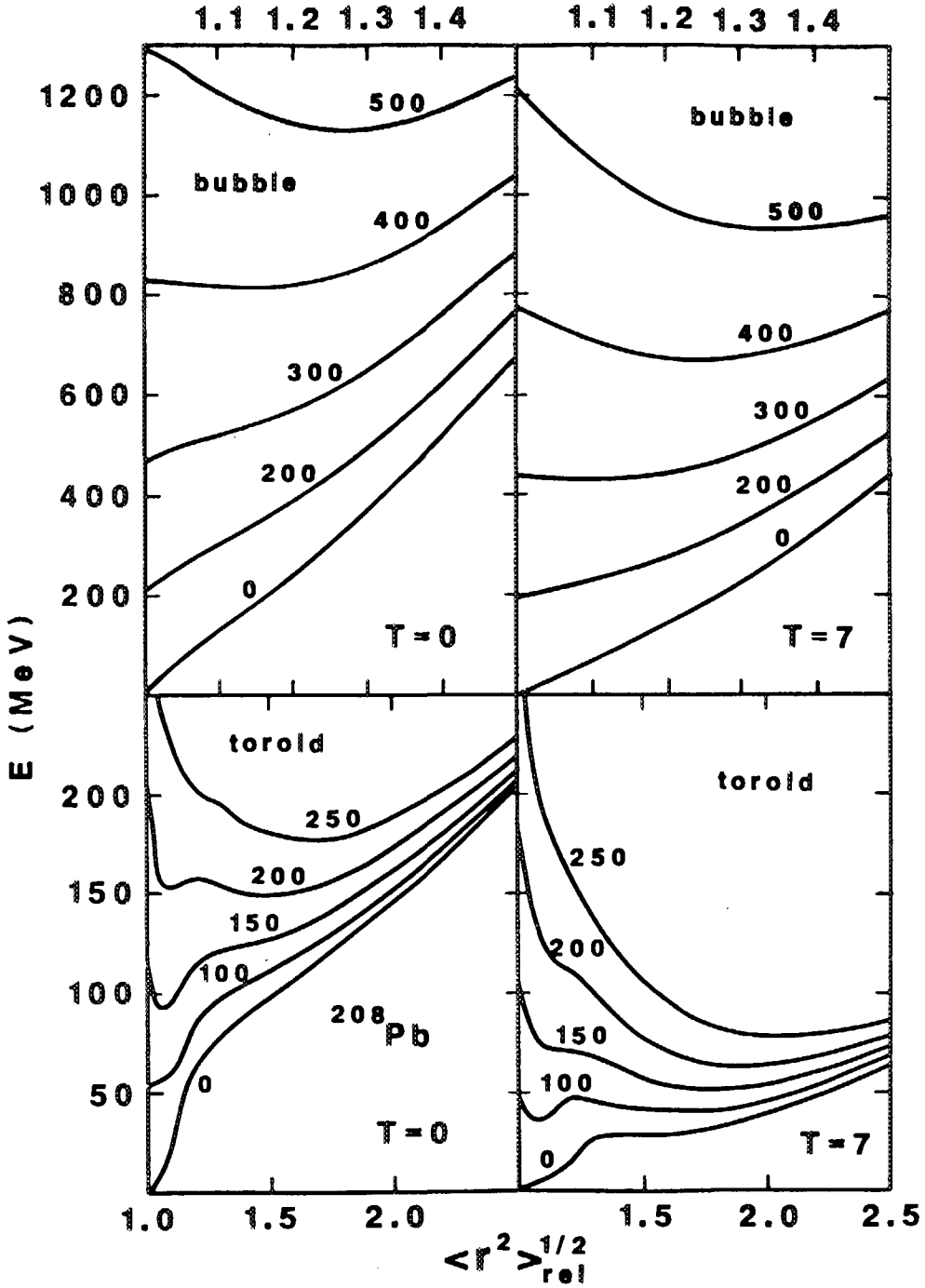

Figure 8

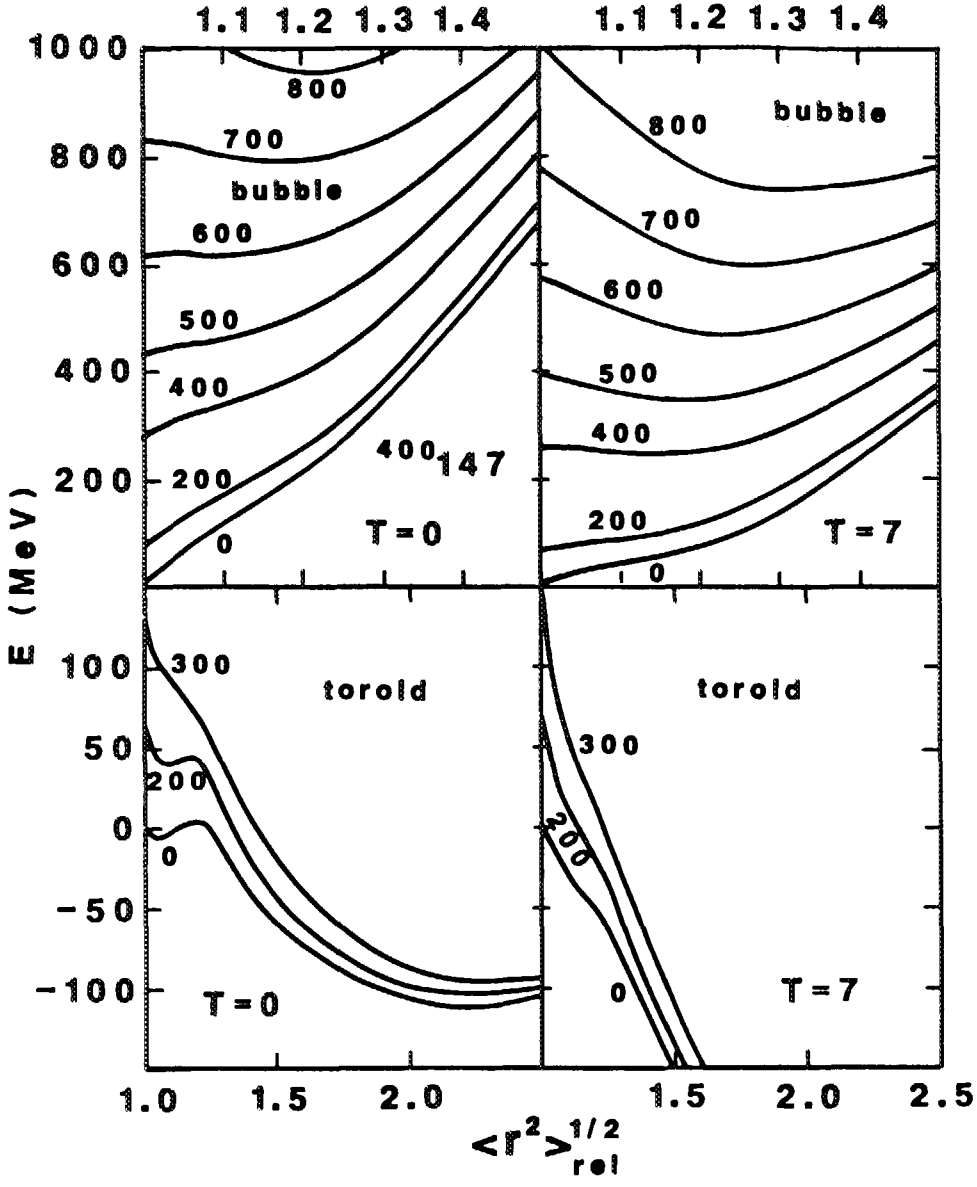

Figure 9

Figure 10

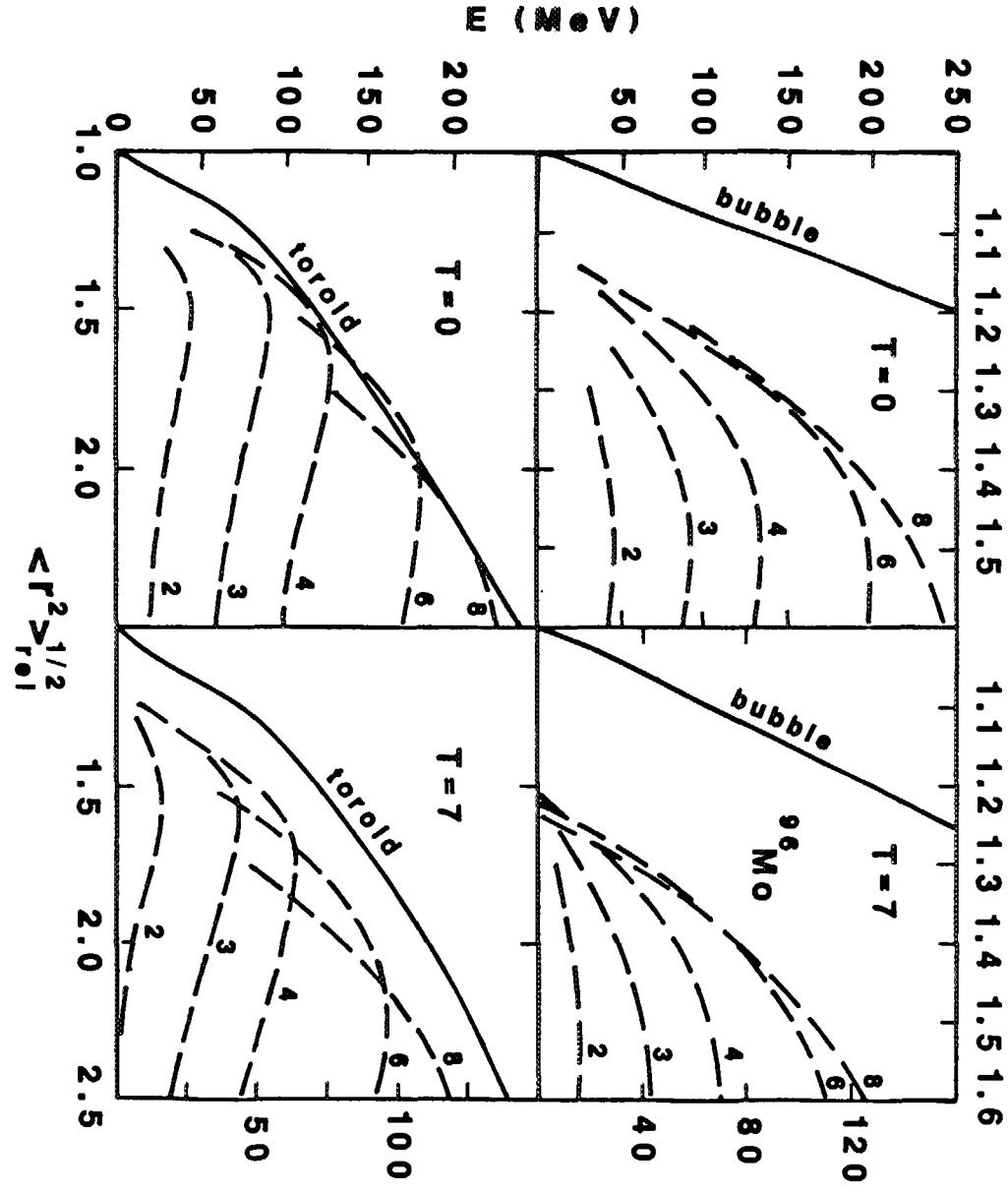

Figure 12

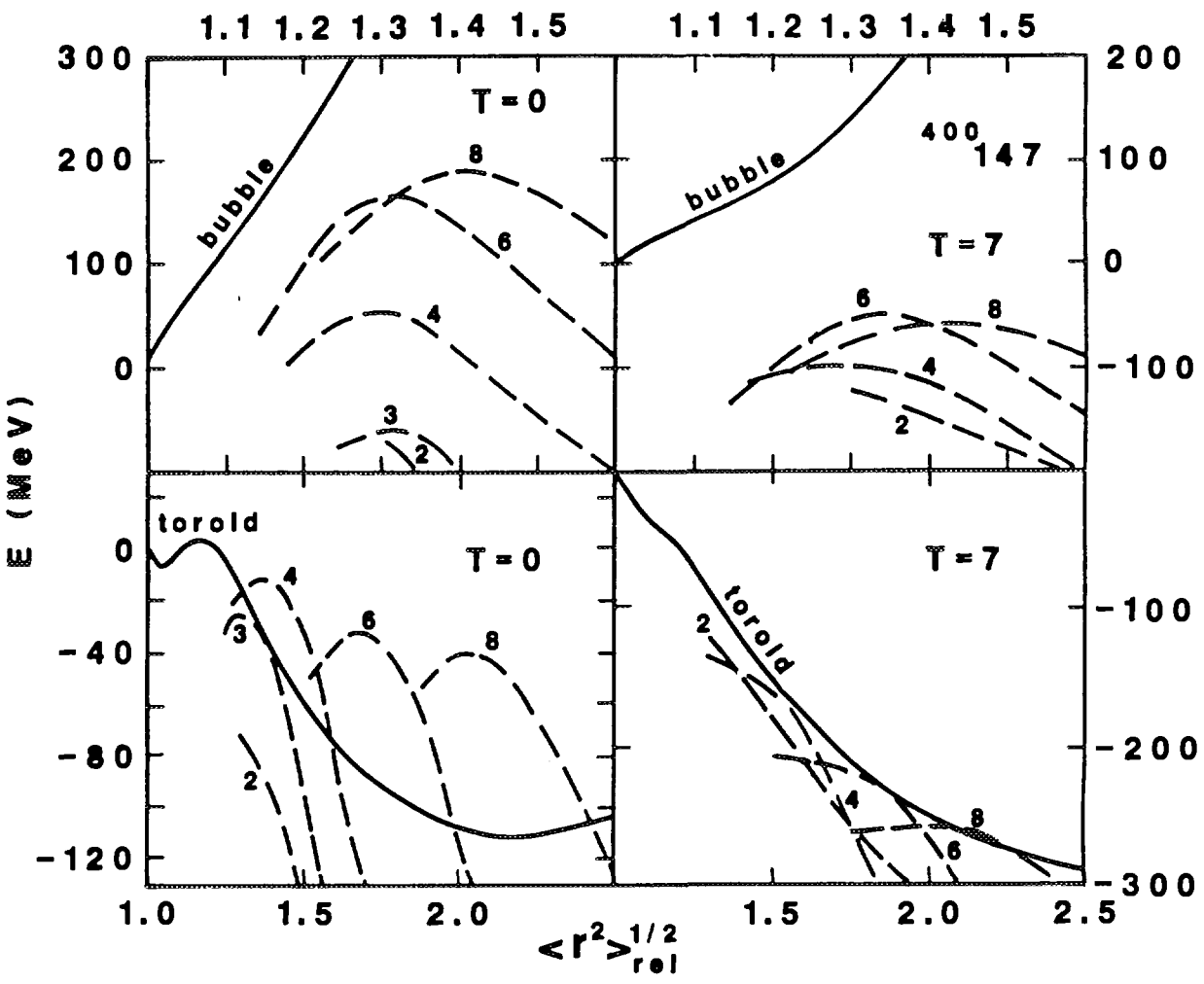

Figure 11